

FILE COPY  
NO. I-W

10085 3/2  
**CASE FILE  
COPY**

**NATIONAL ADVISORY COMMITTEE  
FOR AERONAUTICS**

**REPORT No. 231**

**INVESTIGATION OF TURBULENCE IN WIND  
TUNNELS BY A STUDY OF THE FLOW  
ABOUT CYLINDERS**

**By H. L. DRYDEN and R. H. HEALD**



**WASHINGTON  
GOVERNMENT PRINTING OFFICE  
1926**

**FILE COPY**

To be returned to  
the files of the National  
Advisory Committee  
for Aeronautics  
Washington, D. C.



## AERONAUTICAL SYMBOLS

### 1. FUNDAMENTAL AND DERIVED UNITS

	Symbol	Metric		English	
		Unit	Symbol	Unit	Symbol
Length-----	$l$	meter-----	$m$	foot (or mile)-----	ft. (or mi.).
Time-----	$t$	second-----	$sec$	second (or hour)-----	sec. (or hr.).
Force-----	$F$	weight of one kilogram-----	$kg$	weight of one pound-----	lb.
Power-----	$P$	kg/m/sec-----		horsepower-----	HP.
Speed-----		m/sec-----		mi./hr-----	M. P. H.

### 2. GENERAL SYMBOLS, ETC.

Weight,  $W = mg$ .

Standard acceleration of gravity,

$$g = 9.80665 \text{ m/sec}^2 = 32.1740 \text{ ft./sec.}^2$$

Mass,  $m = \frac{W}{g}$

Density (mass per unit volume),  $\rho$

Standard density of dry air,  $0.12497 \text{ (kg-m}^{-4}\text{-sec}^2\text{) at } 15^\circ\text{C and } 760 \text{ mm} = 0.002378 \text{ (lb.-ft.}^{-4}\text{-sec.}^2\text{)}$

Specific weight of "standard" air,  $1.2255 \text{ kg/m}^3 = 0.07651 \text{ lb./ft.}^3$

Moment of inertia,  $mk^2$  (indicate axis of the radius of gyration,  $k$ , by proper subscript)

Area,  $S$ ; wing area,  $S_w$ , etc.

Gap,  $G$ .

Span,  $b$ ; chord length,  $c$ .

Aspect ratio  $= b/c$ .

Distance from  $c. g.$  to elevator hinge,  $f$ .

Coefficient of viscosity,  $\mu$ .

### 3. AERODYNAMICAL SYMBOLS

True airspeed,  $V$ .

Dynamic (or impact) pressure,  $q = \frac{1}{2} \rho V^2$

Lift,  $L$ ; absolute coefficient  $C_L = \frac{L}{qS}$

Drag,  $D$ ; absolute coefficient  $C_D = \frac{D}{qS}$

Cross-wind force,  $C$ ; absolute coefficient

$$C_c = \frac{C}{qS}$$

Resultant force,  $R$ .

(Note that these coefficients are twice as large as the old coefficients  $L_c, D_c$ .)

Angle of setting of wings (relative to thrust line),  $i_w$ .

Angle of stabilizer setting with reference to thrust line,  $i_t$ .

Dihedral angle,  $\gamma$ .

Reynolds Number  $= \rho \frac{Vl}{\mu}$  where  $l$  is a linear dimension.

e. g., for a model airfoil 3 in. chord, 100 mi./hr., normal pressure,  $0^\circ\text{C}$ : 255,000 and at  $15^\circ\text{C}$ , 230,000;

or for a model of 10 cm chord, 40 m/sec, corresponding numbers are 299,000 and 270,000.

Center of pressure coefficient (ratio of distance of  $C. P.$  from leading edge to chord length),  $C_p$ .

Angle of stabilizer setting with reference to lower wing.  $(i_t - i_w) = \beta$ .

Angle of attack,  $\alpha$ .

Angle of downwash,  $\epsilon$ .



---

---

**REPORT No. 231**

---

**INVESTIGATION OF TURBULENCE IN WIND  
TUNNELS BY A STUDY OF THE FLOW  
ABOUT CYLINDERS**

By **H. L. DRYDEN and R. H. HEALD**  
Bureau of Standards

ADDITIONAL COPIES  
OF THIS PUBLICATION MAY BE PROCURED FROM  
THE SUPERINTENDENT OF DOCUMENTS  
GOVERNMENT PRINTING OFFICE  
WASHINGTON, D. C.  
AT  
10 CENTS PER COPY



## REPORT No. 231

### INVESTIGATION OF TURBULENCE IN WIND TUNNELS BY A STUDY OF THE FLOW ABOUT CYLINDERS

By H. L. DRYDEN and R. H. HEALD

#### INTRODUCTION

With the assistance and cooperation of the National Advisory Committee for Aeronautics the Bureau of Standards has been engaged for the past year in an investigation of turbulence in wind tunnels, especially in so far as turbulence affects the results of measurements in different wind tunnels. At the beginning of the year the research was outlined in some detail by the members of the technical staff of the committee, and so far as has been practicable this outline has been followed. The following pages constitute a report to the committee on the results obtained.

The investigation was planned along two lines, the problem of turbulence being attacked in two directions. In the first place the ultimate effect of turbulence, in which we are interested in practice, is its effect on the measured force on objects subjected to test. Certain types of bodies have been found to be very sensitive to changes of turbulence and have been suggested as indicators of the degree of turbulence present. Spheres and cylinders are the bodies most frequently suggested. Spheres having been already studied at Langley Field and elsewhere, cylinders were proposed as the indicating bodies in the present investigation. The behavior of eight cylinders ranging in diameter from 0.0085 inch to 3 inches has been studied for four turbulence conditions, and the 3-inch cylinder has been studied for a variety of other conditions. As a result of these experiments it has been shown that large effects are produced near the critical region of the Reynolds number when the air passing near the surface of the cylinder is subjected to disturbance.

From a more fundamental point of view we can never be satisfied until we know more definitely the nature of turbulence; in other words, its cause and the exact manner in which it manifests itself as changes in the air speed, direction, and pressure. We can, as a result of our work along this line, report progress and point out the nature of the difficulties encountered. We believe that we have reliable methods of measuring changes in static pressure, and we have obtained one positive result, namely, that although as shown by measurements with a Taylor yaw-head there seems to be no twist of the air stream produced by the propeller, there is a definite pattern of pressure changes produced by the blades of the propeller and following it in its revolution. The changes in static pressure are of the order of 2 or 3 per cent of the velocity pressure. With impact tubes we have so far not been able to eliminate variations characteristic of the measuring instrument, and on this account the more difficult problem of studying changes of direction by means of a recording yaw meter has not been attacked.

This in brief is a summary of the lines along which we have been working. The following sections describe in detail the more important results obtained.



PART I  
FORCE MEASUREMENTS ON CYLINDERS

WIND TUNNEL

The measurements of the resistance of cylinders were carried out in the 54-inch wind tunnel of the Bureau of Standards. This tunnel is of the room return type and consists of a faired entrance 4.3 feet long, a straight section 25.3 feet long, and an exit cone 15.1 feet long. The straight section is of octagonal cross section, the distance between opposite faces being 54 inches. The diameter at the exit end is 9 feet. Two honeycombs are installed within the tunnel, one at each end of the straight section. The front honeycomb is of hexagonal cells, 3.25 inches between opposite faces and 18 inches long. The metal of which the honeycomb is made is 0.03 inch thick. The rear honeycomb is made by piling 12-inch sections of 3-inch sheet-metal tubing against a grid of retaining wires. The experimental station at which the cylinders were placed is 9.6 feet downstream from the front honeycomb.

The room in which the tunnel is centrally located is 68.5 feet long, 28.3 feet wide, 18 feet high. One room, honeycomb made up of 1-inch mailing tubes, 4 inches long, piled between retaining screens, is installed in the plane of the propeller.

SPEED MEASUREMENT

Air speeds are ordinarily measured by means of a static plate 4.5 feet upstream from the experimental station, standardized in terms of the readings of a Pitot tube placed at the position to be occupied by the model. When screens are used close to the experimental station, it is usually difficult to obtain a satisfactory calibration because of the nonuniform distribution of velocity across the tunnel. We feel that it is better to measure the average speed ahead of the screen at a place where the speed is nearly constant over the cross section. Since the average speed at all sections of the tunnel must be approximately the same, this procedure gives a close approximation to the average speed at the cylinder. There is one source of error, namely, the possibility that the distribution near the wall may be greatly modified, so that although the average speed over the entire cross section remains constant the average speed over the central part of the tunnel may be changed. The results seem to indicate that this effect is not present to any appreciable extent.

Our standard for speed measurement in the measurements here reported was a Pitot tube mounted on wires 2 feet ahead of the screen, where screens are used, and midway between the axis of the tunnel and the wall. In measurements with no screens present the tube was placed 2 feet 8 inches ahead of the balance axis. Speeds ranged from 20 to 80 feet per second and occasionally to 100 feet per second when the steadiness of the balance permitted.

CYLINDERS

Eight cylinders were used, ranging in diameter from 0.0085 inch to 3 inches. The exact diameters were as follows: 0.0085 inch, 0.063 inch, 0.156 inch, 0.250 inch, 0.500 inch, 0.983 inch, 2.001 inches, and 3.149 inches. The smallest cylinder was a piece of ordinary steel wire; the next four were drill rods, and the last three were pieces of brass tubing. On the curve sheets the cylinders are designated by their approximate diameters 0.0085 inch,  $\frac{1}{16}$  inch,  $\frac{5}{32}$  inch,  $\frac{1}{4}$  inch,  $\frac{1}{2}$  inch, 1 inch, 2 inches, 3 inches. The length actually subject to the force of the air stream was about 30 inches, but the conditions approximated those of two-dimensional flow as explained in the section on balances.

SCREENS

Two screens were used as sources of artificial turbulence, one a screen of  $\frac{1}{16}$ -inch mesh, the individual wires being 0.011 inch in diameter, the other a screen of  $\frac{1}{2}$ -inch mesh, the individ-



ual wires being 0.047 inch in diameter. The  $\frac{1}{2}$ -inch mesh screen was formed of wires soldered together and the junction points were somewhat enlarged. The screens were used at two distances, namely, 36 inches and 8 inches from the balance axis.

#### ARRANGEMENT FOR MEASURING FORCES

The sketch in Figure 1 shows the two methods used for force measurements. In both methods the supports for the wires or cylinders were inclosed within wind shields (see fig. 1), the wind shields being long enough to extend outside the region of reduced speed near the walls. This method of approximating two dimensional flow was used in preference to guards in order that similar methods might be used for all cylinders. Measurements on the 1-inch cylinder mounted in a horizontal position with end guards checked the measurements on the set-up finally adopted within 2 per cent.

In the case of the two smallest cylinders (figs. 1A and 1B) the air force was determined by measuring the deflection. The wires were kept under a known tension by means of a weight applied at the lower end, and end constraints were eliminated by the use of short sections of fine wire at the top support and over a pulley at the bottom. The drag equals eight times the product of tension by deflection at the center, divided by the length if the deflection is small.<sup>1</sup>

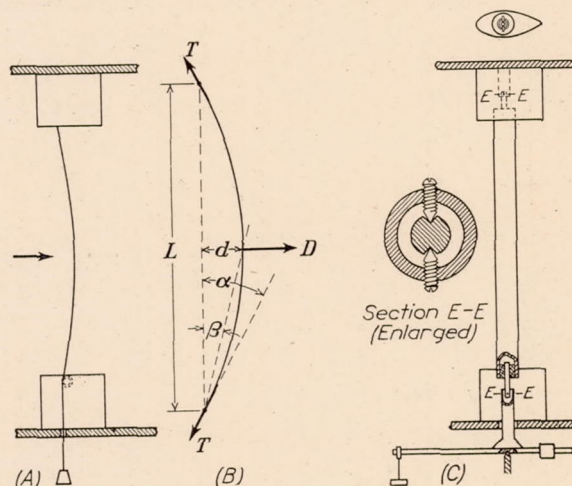


FIG. 1

The larger cylinders were supported from the tunnel roof on two pivot bearings (fig. 1C) in such a manner as to be free to rotate about the line of the pivots in a plane parallel to the wind direction. The lower end was attached to the top of the N. P. L. type balance by a similar connection. Only a part of the force acting on the cylinder is communicated to the balance. Direct calibrations by loads applied horizontally at the centers of the cylinders gave values of the ratio of balance reading to applied load checking the computed value 0.188 within 1 per cent. It was found possible to adjust the sensitivity of the N. P. L. type balance to values satisfactory for the six large cylinders, although the forces varied from about 0.03 pound to over 5 pounds.

<sup>1</sup> In the sketch (fig. 1B) in the condition of equilibrium

$$D = 2T \sin \alpha$$

where  $D$  is the total drag on the wire,  $T$  is the tension, and  $\alpha$  the angle of the tangent at the end, made small by using a sufficiently high tension so that  $\sin \alpha$  equals  $\alpha$  very closely. With a small deflection the wire may be assumed to take a circular form in which case  $\alpha = 2\beta$  where  $\beta = \frac{d}{L/2}$   $d$  being the deflection at the center and  $L$  the chord length. Hence

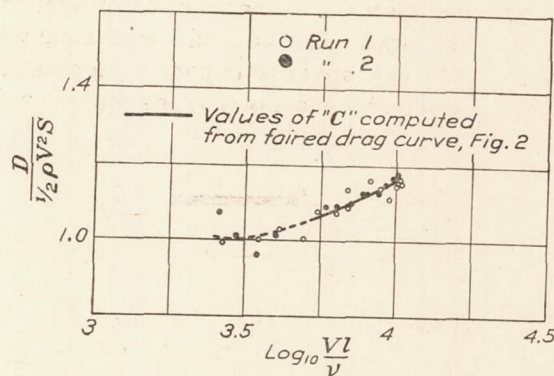
$$D = \frac{8Td}{L}$$

Closer analysis shows that the term neglected in assuming  $\alpha$  small and a circular form is of the order  $16 \frac{d^3}{L^2}$  as compared with 1.



## RESULTS OF TESTS

The results are expressed in the form of nondimensional coefficients plotted against the common logarithm of the Reynolds number. The coefficient is defined by the relation  $D = CSq$ ,  $D$  being the drag on the cylinder,  $S$  the product of cylinder diameter by the length exposed to the wind stream,  $q$  the velocity pressure  $\frac{1}{2}\rho V^2$  and  $C$  the coefficient. The Reynolds number is defined as  $\frac{Vl\rho}{\mu}$  where  $V$  is the wind speed,  $l$  the cylinder diameter,  $\rho$  the density of the air, and  $\mu$  the viscosity of the air.

FIG. 2.—Resistance of  $\frac{1}{4}$ -inch cylinder, open tunnelFIG. 3.— $\frac{1}{4}$ -inch cylinder, open tunnel

The curves shown in Figures 4, 5, 6, and 7 are each computed from average curves representing the force measurements plotted against wind speed. A typical curve of this type is shown in Figure 2. Each individual observation has been represented by plotting the coefficient against the Reynolds number in Figure 3. It will be noticed that individual observations depart from the mean curve by a maximum of 3 per cent. This is true for all cylinders, and the example shown is typical. Results for speeds below 40 feet per second are less accurate than those for speeds above 40 feet per second and are indicated by dotted curves.

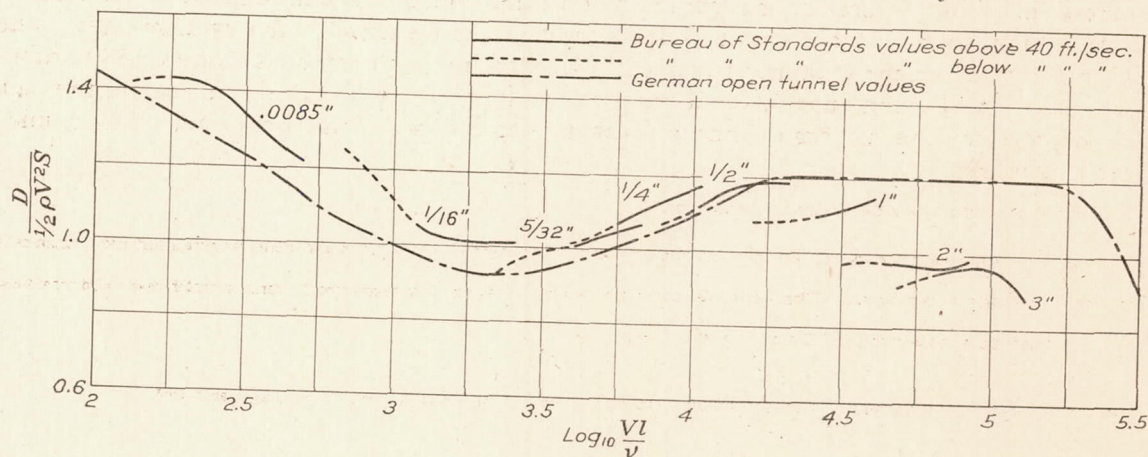
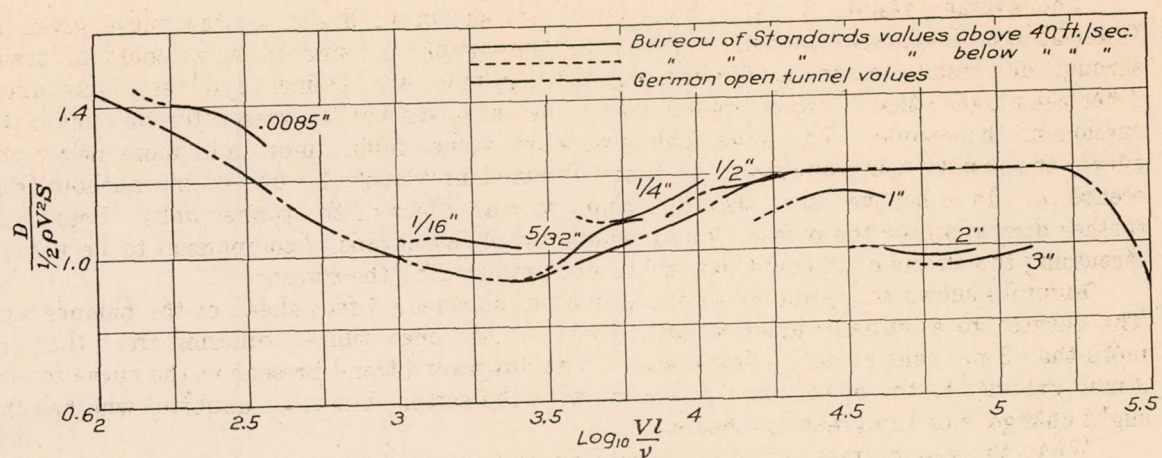
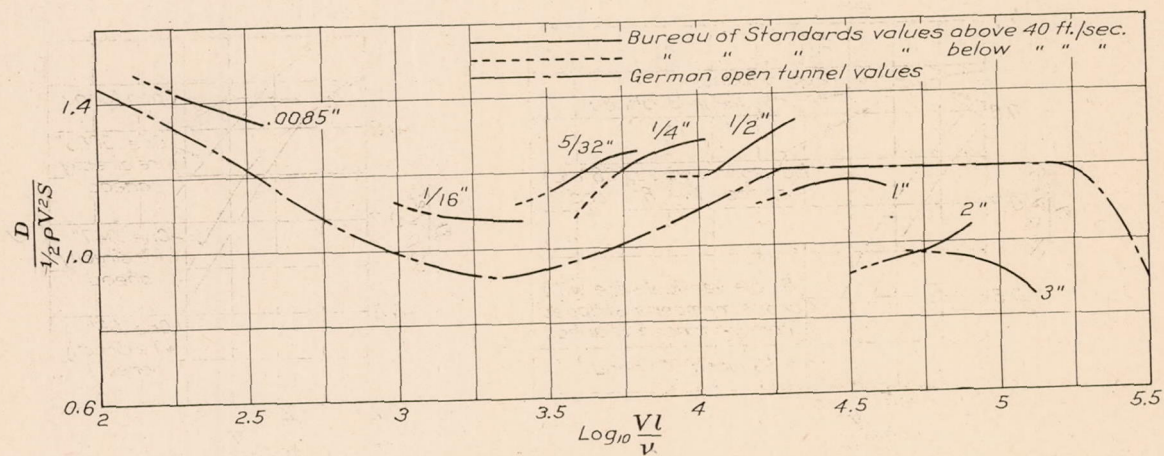
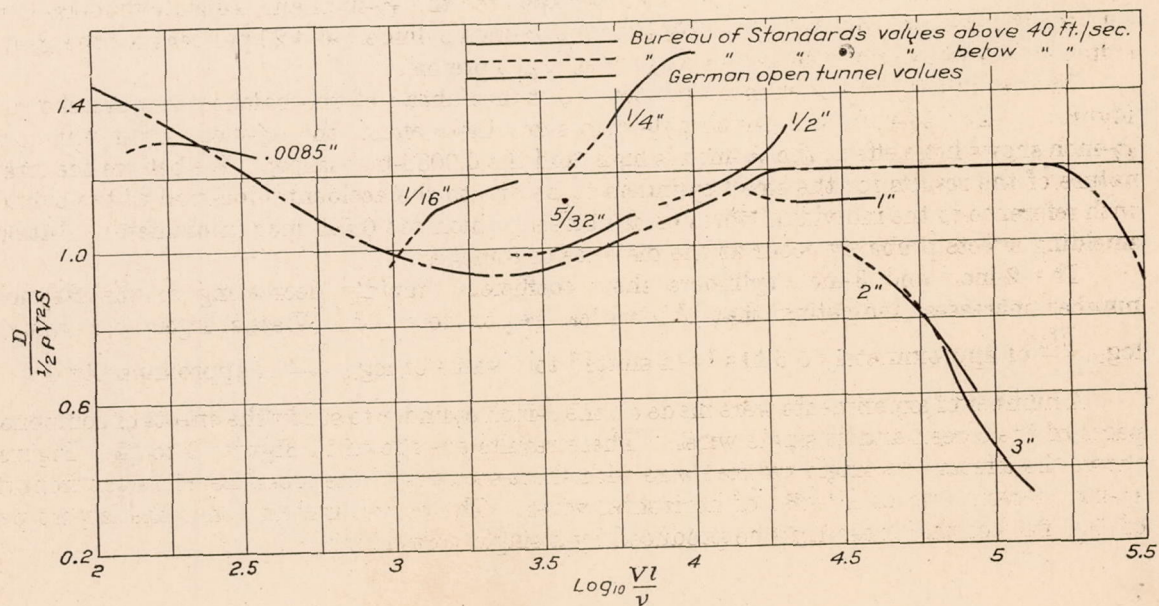


FIG. 4.—Cylinders in open tunnel




 FIG. 5.—Cylinders 3 feet behind  $\frac{1}{8}$ -inch mesh screen

 FIG. 6.—Cylinders 8 inches behind  $\frac{1}{8}$ -inch mesh screen

 FIG. 7.—Cylinders 8 inches behind  $\frac{1}{2}$ -inch mesh screen



The average results for the open tunnel are shown in Figure 4, the curve given by Wieselsberger (Reference 1) being inserted for comparison. A smooth curve could be drawn through our results for the 0.0085-inch,  $\frac{1}{16}$ -inch,  $\frac{5}{32}$ -inch, and  $\frac{1}{4}$ -inch cylinders, lying about 7 per cent higher than Wieselsberger's curve. We shall discuss the reason for this under discussion of the results. The larger cylinders show values falling more and more below this curve, the results being analogous to those obtained previously by one of the authors (Reference 2). It is believed that this is in some way an effect of the tunnel walls. Passing by further discussion for the present, these results are the standards of comparison to be used in discussing the effects of the artificial turbulence produced by the screens.

Figure 5 shows the results with the  $\frac{1}{16}$ -inch mesh screen 3 feet ahead of the balance axis. The curves are essentially identical with those for the open tunnel, differing from them by more than 3 per cent at only a few places. The downward trend present in the curve for the 3-inch cylinder in the open tunnel is absent with the screen, but it is doubtful whether this slight change is of any great significance.

When the  $\frac{1}{16}$ -inch mesh screen is moved closer to the balance axis the results in Figure 6 are obtained. The 0.0085-inch, 2-inch, and 3-inch cylinders are unaffected. The values for

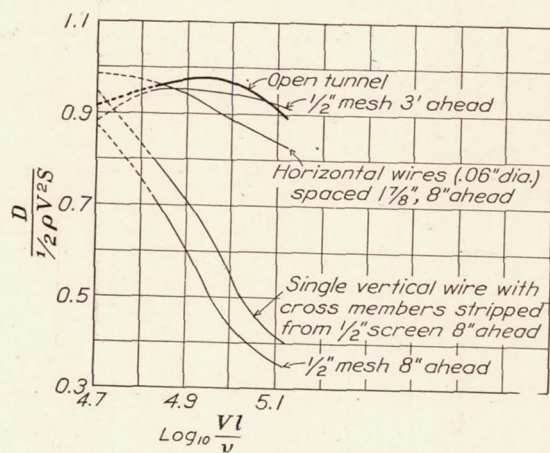


FIG. 8.—3-inch cylinder

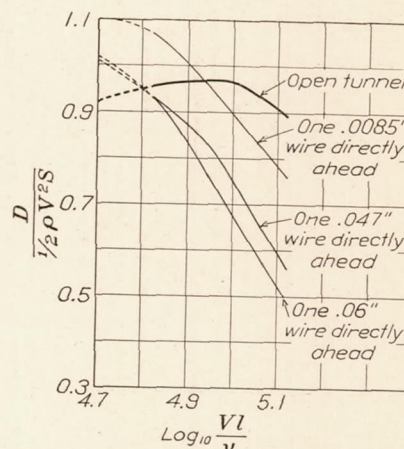


FIG. 9.—3-inch cylinder; wires 8 inches ahead

the other cylinders are higher by about 6 per cent for the  $\frac{1}{16}$ -inch and 1-inch cylinders, 8 per cent for the  $\frac{1}{2}$ -inch cylinder, 14 per cent for the  $\frac{1}{4}$ -inch cylinder, and 20 per cent for the  $\frac{5}{32}$ -inch cylinder. We have no explanation for this effect at present.

The results for the  $\frac{1}{2}$ -inch mesh screen 8 inches ahead of the balance axis are shown in Figure 7. The  $\frac{1}{2}$ -inch and 1-inch cylinders show little effect, the  $\frac{1}{4}$ -inch is very high, the  $\frac{5}{32}$ -inch shows little effect, the  $\frac{1}{16}$ -inch is high, and the 0.0085-inch is low. We believe the erratic nature of the results for the small cylinders to be due to the accidental location of the cylinder with reference to the individual wires of the screen, which are 0.047 inch in diameter. Marked shielding effects probably occur at the distance of 8 inches.

The 2-inch and 3-inch cylinders show coefficients rapidly decreasing as the Reynolds number increases, indicating that the critical region found by Wieselsberger at a value of  $\log_{10} \frac{Vl\rho}{\mu}$  of approximately 5.5 has been shifted to a value of  $\log_{10} \frac{Vl\rho}{\mu}$  of approximately 4.7.

A number of experiments were made on the 3-inch cylinder to study the effects of component parts of the screen and of single wires. These results are shown in Figures 8 to 12. Figure 8 shows the effects of a single vertical wire with short sections of the cross members cut from the  $\frac{1}{2}$ -inch screen, and of a series of horizontal wires. The curves indicate that the largest part of the effect of the screen may be produced by a single vertical wire.



As a result of this observation a fairly complete study was made of the effects of single wires in various positions. Figure 9 shows the effect of varying the wire diameter; large diameter wires producing the largest effect. At low Reynolds numbers, however, the wire increases the resistance. Figure 10 shows the results of a traverse along a line perpendicular to the plane of cylinder axis and wind direction. The effect practically disappears when the wire is moved one-half inch from a position directly ahead. Figure 11 shows the results of a longitudinal traverse. The effect is greatest at distances of 8 to 14 inches from the cylinder axis. The decreasing effect at smaller distances is presumably due to the decrease in the intensity of the disturbance in the region of reduced speed near the cylinder. The group of curves indicates that the critical region is shifted when the air passing close to the surface of the cylinder is affected, and if there is no disturbance of this air the effects are small.

Figure 12 shows that similar results are obtained when the boundary layer is disturbed by small projections on the surface of the cylinder and that effects may be produced at distances much greater than 8 inches by increasing the intensity of the disturbance, as, for example, by allowing small tags to flutter in the wind stream.

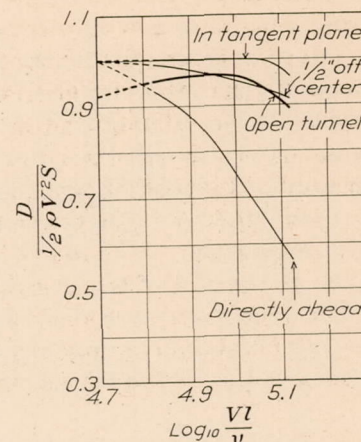


FIG. 10.—3-inch cylinder. Single .047-inch vertical wire 8 inches ahead

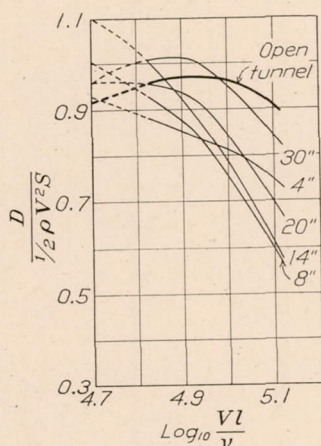


FIG. 11.—3-inch cylinder. Single .047-inch wire directly ahead

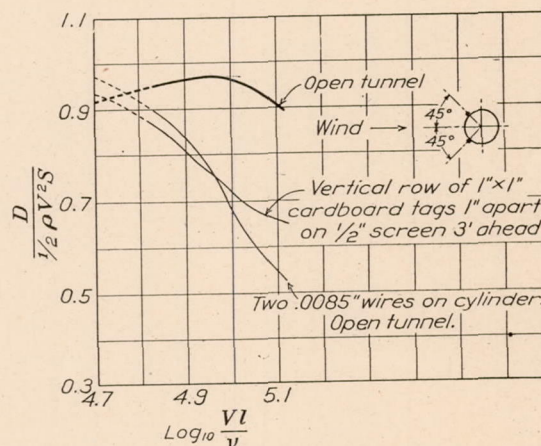


FIG. 12.—3-inch cylinder

### DISCUSSION OF THE OBSERVED CYLINDER DRAG

We have called attention to the fact that our results for the smaller cylinders are about 7 per cent higher than those of Wieselsberger. The results of Relf (Reference 3) are in general about 3 per cent higher than those of Wieselsberger. We believe that the differences are due to the differences in the methods used to obtain two-dimensional flow. In Relf's experiments a correction was made for the effect of the ends of the wires by taking the measured force as applying to a wire four diameters shorter than the actual wire tested. For the smallest wires a number of wires were mounted in a rectangular frame, in which case a fairly large correction was necessary for the resistance of the frame, and its effect in modifying the flow is unknown. In Wieselsberger's experiments cylinders less than 0.3-inch in diameter were hung on a long wire from the ceiling of the experimental chamber<sup>2</sup> and stretched across the air stream, being kept in tension by a weight below. The resistance was computed from the deflection of the system as a pendulum. The length exposed to the stream was somewhat indefinite because of the velocity

<sup>2</sup> In the Gottingen tunnel the air stream is not inclosed at the experimental chamber.



changes near the boundary of the stream. In our own experiments we have shielded the cylinders in the region of decreased velocity near the wall, but there remains the possibility of disturbances due to the wind shields. The resistance of small wires under conditions of two-dimensional flow is therefore uncertain by about  $\pm 3$  per cent.

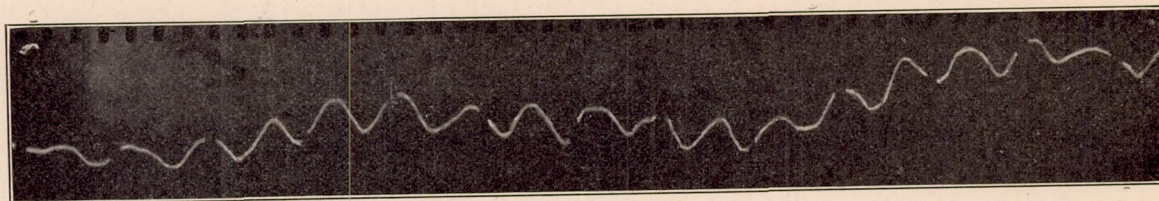
If the models and their mountings were geometrically similar and if there were no effect of the tunnel walls, the values for all the cylinders would be expected to lie on a smooth curve. In the case of the larger cylinders the departures from such a smooth curve are very marked. It is quite possible that the departure is due to an effect of the walls of the tunnel, since the 1-inch cylinder, for example, blocks off about 2 per cent of the tunnel area, but it is difficult to understand why some such effect in the opposite direction was not found in Wieselsberger's experiments in an open-air stream, for he found the law of similarity to hold even when the cylinder occupied as much as 15 per cent of the area of the wind stream. Relf also obtained consistent results when the cylinder diameter was about 3 per cent of the length of the side of his square tunnel, although the ratio of the area occupied by the cylinder to the area of the wind stream was much less because a short cylinder was used.



## PART II

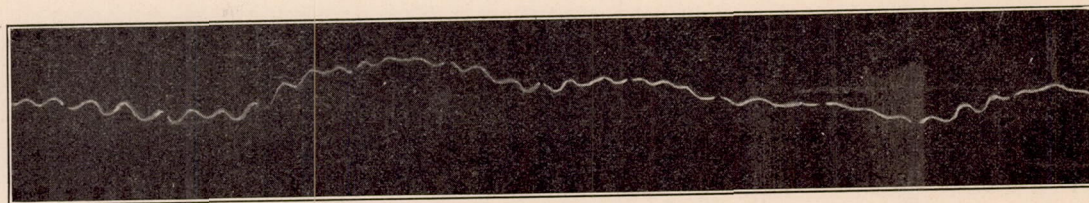
### MEASUREMENTS OF EDDY FREQUENCY BEHIND CYLINDERS

It was shown by Karman (Reference 4) that vortices break off fairly regularly behind a circular cylinder in the range of Reynolds numbers here studied, and the frequency with which they break off has recently been measured by Relf and Simmons (Reference 5). In order to measure the frequency in their experiments, a short platinum wire heated to redness was mounted



A. Pressure variation due to eddies behind 3.15-inch cylinder, no screen. Air speed, 65.5 ft./sec. Time between breaks, 0.0296 seconds.  
Frequency, 47.3 per second.  $\frac{\sim D}{V} = 0.19$

$\text{Log}_{10} R = 5.033$



B. Pressure variation due to eddies behind 3.15-inch cylinder,  $\frac{1}{2}$ -inch mesh screen 8 inches ahead. Air speed, 78.2 ft./sec. Time between breaks, 0.0308 sec.  
Frequency, 97.5 per second.  $\frac{\sim D}{V} = 0.327$

$\text{Log}_{10} R = 5.11$

FIG. 13

behind the cylinder and the heating circuit coupled by means of a transformer to a circuit in which a string galvanometer was placed. The galvanometer was tuned to resonance with the oscillations of the heating current produced by the velocity changes near the hot wire. The galvanometer was then connected to a single-phase alternator and the speed of rotation of the alternator varied until resonance was again obtained. The alternator speed gave the eddy frequency directly. The most striking feature of their results was the occurrence of a rapid rise in frequency as the critical region of Reynolds number (where the resistance coefficient falls very rapidly) was reached.

We made a few measurements of eddy frequency to check the occurrence of this rise in frequency when the critical region is artificially displaced, and, as would be expected, found the rise to take place. The experimental arrangement was quite simple. A standard Pitot tube was placed about one diameter behind the cylinder and slightly inside the shadow of the cylinder. The static openings of the Pitot were connected to the diaphragm pressure gauge described in Part III of this report and the pressure variations observed photographically. Typical records are shown in Figure 13 A and B, the upper record under conditions of flow corresponding to Reynolds numbers below the critical region, the lower under conditions of flow

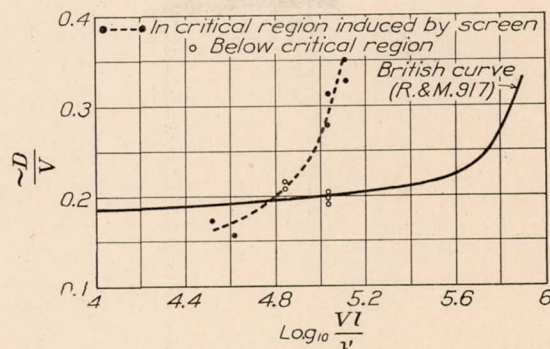


FIG. 14.—Frequency of eddies behind circular cylinders



corresponding to Reynolds numbers above the critical region, obtained by the use of the  $\frac{1}{2}$ -inch-mesh screen 8 inches ahead. The photographic records show that the eddies come off periodically for short-time intervals, but disturbances in the regular course are quite marked, especially when the flow is critical. Figure 14 shows a comparison of our results with those obtained by Relf and Simmons. The points marked as being below the critical region were obtained in the tunnel with the usual honeycombs; those marked as in the critical region, behind the  $\frac{1}{2}$ -inch-mesh screen 8 inches ahead. The presence of this screen induces the critical flow at a Reynolds number lower than normal.



### PART III

## MEASUREMENT OF PRESSURE VARIATIONS

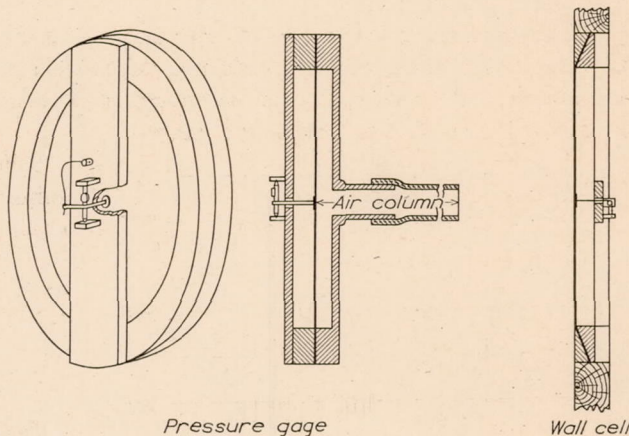
### INTRODUCTION

The departures of the air streams of our wind tunnels from the ideal condition of steady and uniform flow, which we group under the name of turbulence, are resolvable ultimately in terms of variations of speed, direction, and static pressure. The direct measurement of turbulence requires the measurement of these variations, a task to which some attention has been given. All of the measurements reduce ultimately to measurements of pressure variations, so that a desirable instrument is a sensitive high-frequency pressure gauge.

The frequencies with which we are concerned are high compared with the frequency of the balance used for force measurements; in other words, of the order of 10 per second and higher. An upper limit is rather hard to fix, but we have attempted to study the range from about 5 per second to 100 per second.

### DESCRIPTION OF GAUGE

The fluctuation is rather small, amounting to less than 5 per cent of the velocity pressure; in other words, to less than one-eighth of an inch of water at an air speed of 100 feet per second. The gauge must therefore be rather sensitive, and we have used a diaphragm of rolled aluminum 0.001 inch in thickness and 4 inches in diameter. The motion of the diaphragm is magnified by the arrangement shown in figure 15. A ribbon attached to the center of the diaphragm passes over a shaft and is kept taut by a spring. The shaft carries a mirror whose motion may be recorded photographically. The necessity for sensitiveness, leading to a system of low stiffness, reduces the natural frequency of the system, but there is no difficulty in obtaining a natural frequency of about 500 per second as shown by actual measurement.



Pressure gage

FIG. 15

Wall cell

### CHARACTERISTICS OF GAUGE SYSTEM

However, to measure the pressure at the static opening of a Pitot tube, the gauge is necessarily placed some distance away, and a connection must be made by rubber tubing. It was found very early in our work that when  $\frac{1}{4}$ -inch tubing was used no disturbance of high frequency was transmitted through the tubing. We were thus led to the use of  $\frac{1}{2}$ -inch tubing and in some special experiments to connections of diameter as large as  $1\frac{1}{2}$  inches. After many records had been taken in the 54-inch tunnel the equipment was moved to the 10-foot outdoor tunnel and a number of records taken there. The records were so similar in character as to indicate that they were due to the measuring instrument rather than to the tunnel, and further experiment showed that the character of the record depended primarily on the length and diameter of tubing connecting the tube to the gauge.

We had, in some preliminary work, tested the system for resonance by connecting the gauge to a chamber in which a piston was moved back and forth and noting the amplitude shown by the gauge. Further investigation showed that this procedure gave misleading results because of the modification of the end of the air column at the pump. (Fig. 16.) More



reliable results were obtained by inducing the vibration through a T connection, the gauge being connected to the leg of the T, and the pump to one of the arms, the other arm being left open.

By this method the curve shown in figure 17 was obtained. With 39.4 inches of  $\frac{1}{2}$ -inch tubing the natural frequency of the air column is 20 per second. It will be seen that the frequency varies with the length according to the law

$$\frac{1}{n^2} - \frac{1}{n_0^2} = 0.000064L$$

where  $n_0 = 84.6$ ,  $n$  being the frequency and  $L$  the length. As nearly as can be judged by ear  $n_0$  is of the order of magnitude of the frequency of the gauge box as a resonator. Our gauge system forms a type of resonator whose frequency depends on the conductance of the outlet (Reference 6), and the conductance in turn is approximately proportional to the re-

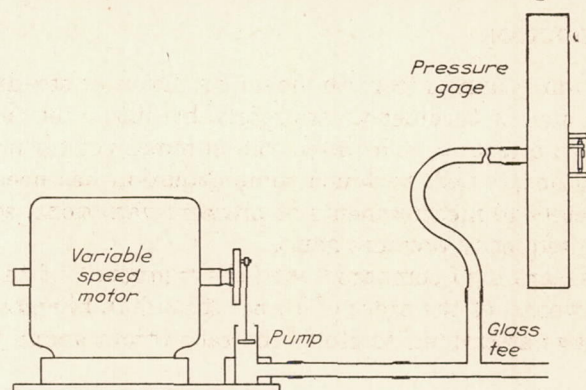


FIG. 16.—Apparatus for measurement of resonance frequencies

reciprocal of the length of the attached tubing, when the length is large in comparison with the diameter of the tubing.

Unfortunately this range of frequency is exactly the range in which we are interested, for the frequency with which a propeller blade passes a fixed point lies within this range for all air speeds. The gauge system, therefore, as a whole is not very suitable for the investigation of disturbances in this frequency range.

Systems of this type have been investigated in some detail by L. F. Simmons and F. C. Johansen at the National Physical Laboratory (Reference 7). A similar variation of resonance frequency with length of tubing was found.

#### WALL CELL

Having no success in getting a system of satisfactory sensitiveness and high natural frequency we then constructed a gauge suitable for measuring static pressure at the wall of the wind tunnel directly. This consisted (fig. 15) of a diaphragm placed flush with the tunnel wall, the clamping ring being let into the wall so that there were no projections to disturb the flow. The mirror system was arranged as in the other gauge and the diaphragm left without air chambers on either side. We have every reason to believe that this wall cell, as we have called it, gives an accurate reproduction of the changes in static pressure at the wall of the tunnel. Figures 18 A, B, and C show records obtained with this cell. The amplitude shown represents about 2 to 3 per cent of the velocity pressure. The frequencies are as indicated.

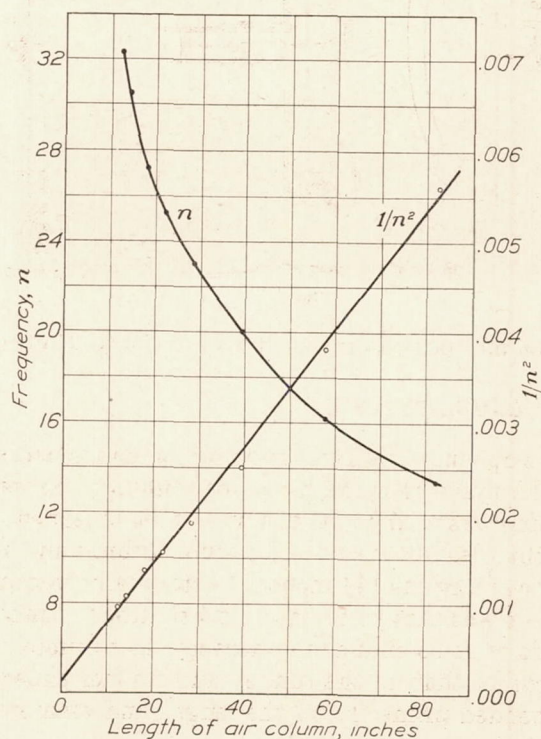


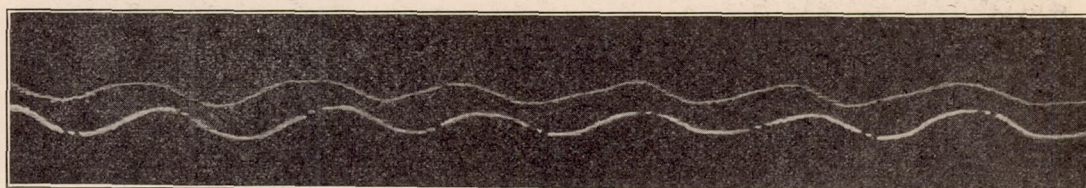
FIG. 17.—Resonance frequencies of gauge and attached tubing

The records shown were obtained by reflecting a beam of light from the mirror of the gauge through a lens to a camera. Motion-picture film was used and was moved past the open shutter at a suitable rate. The beam of light was cut off periodically by a sector on the shaft of a motor and the speed of this timing motor observed by a direct connected tachometer.

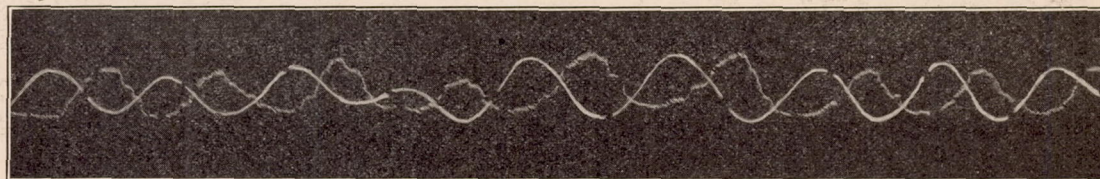


## STATIC PLATE RECORDS

The second trace on the records shown in figure 18 was made by a system consisting of the gauge first described connected to a static plate mounted just below the wall cell. A comparison of the records shows the behavior of the gauge system. The predominant frequency observed is that at which a propeller blade passes a fixed point. The four-blade propeller, which draws air through the tunnel, exerts the greatest pull just behind the blades, and each time a blade passes there is an impulse given to the air behind it. These are the impulses recorded. These pressure variations set up forced oscillations in the gauge system, and the



A. Comparison of wall cell (fainter record) and wall plate. Air speed, 40 ft./sec. Time breaks, 0.034 sec. apart. Wind tunnel motor, 300 revolutions per minute. Frequency of blade impulses, 20 per second. Length of air column on wall plate, 19.3 inches; natural frequency, 26.8 per second



B. Comparison of wall cell (fainter record) and wall plate. Air speed, 53.3 ft./sec. Time breaks, 0.03 sec. apart. Wind tunnel motor, 400 revolutions per minute. Frequency of blade impulses, 26.6 per second. Length of air column on wall plate, 19.3 inches; natural frequency, 26.8 per second



C. Comparison of wall cell (fainter record) and wall plate. Air speed, 60 ft./sec. Time breaks, 0.03 sec. apart. Wind tunnel motor, 450 revolutions per minute. Frequency of blade impulses, 30 per second. Length of air column on wall plate 19.3 inches; natural frequency, 26.8 per second.

NOTE.—The relative phase change on passing through resonance frequency

FIG. 18

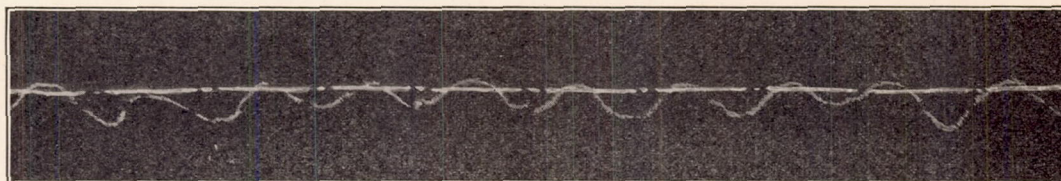
well-known behavior of such a system near its natural frequency is shown. The gauge system is only one-third as sensitive as the wall-cell system, because of differences in path of the light beams and the presence of an additional reflection in the path of the wall-cell beam, yet the gauge system shows as large an amplitude on the record as the wall cell. Furthermore, when the impressed frequency is lower than the natural frequency of the gauge system the oscillations are in phase; when equal to the natural frequency the records differ in phase by one-quarter period, and when above the natural frequency they are in opposite phase. (Reference 8.) We may remark parenthetically that the small amplitude of the pressure variations produced by eddies, shown on the record in figure 13, is due to the fact that the eddy frequency is near 100 as compared with a natural frequency of the gauge system of about 10.

## PITOT TUBE RECORDS

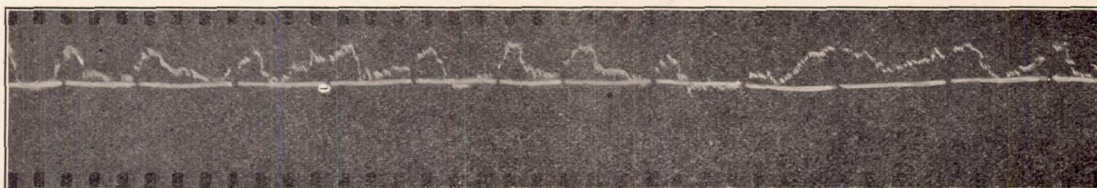
When attempts were made to use Pitot tubes placed in the air stream, especially when impact openings were used, a more serious difficulty arose. This was the vibration of the air column with its own natural frequency, induced by the air flow around the tube. When the



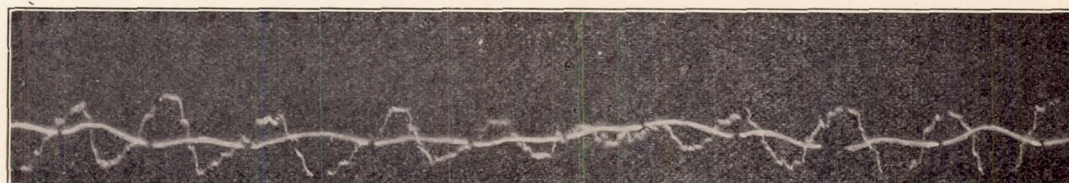
static of the standard Pitot tube is used, the effects were not evident, but as shown in figure 19 A and B nothing of high frequency was transmitted. The damping was large, and the natural frequency very low. When a larger Pitot tube was used with  $\frac{1}{2}$ -inch connections, we found at low and moderate speeds the blade impulses coming through, accompanied by an oscillation of frequency near 11 per second. At high speeds this low frequency alone (fig. 19 D) was recorded with very large amplitude. This frequency is lower than that shown by figure 17, probably because of the additional resistance of the small static openings of the tube. We have not as



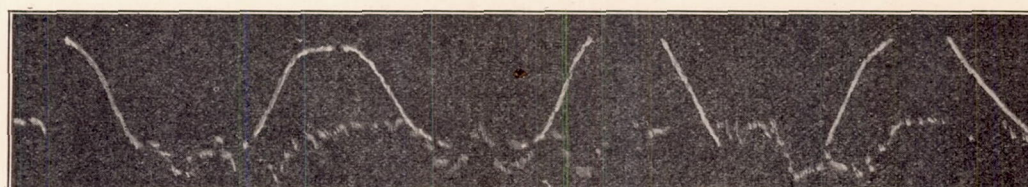
A. Comparison of static of standard Pitot tube and wall cell; 43.3 inches of  $\frac{1}{4}$ -inch tubing; 60 ft./sec. Time breaks, 0.034 sec. apart. Wind tunnel motor, 450 revolutions per minute. Frequency of blade impulses, 30 per second. Compare with Fig. 18C



B. Comparison of static of standard Pitot tube and wall cell; 43.3 inches of  $\frac{1}{4}$ -inch tubing; 66 ft./sec. Time breaks, 0.03 sec. apart. Wind tunnel motor, 495 revolutions per minute. Frequency of blade impulses, 33 per second



C. Comparison of static of large Pitot tube and wall cell; 43.3 inches of  $\frac{1}{2}$ -inch tubing; 66 ft./sec. Time breaks, 0.03 sec. apart. Wind tunnel motor, 495 revolutions per minute. Frequency of blade impulses, 33 per second



D. Comparison of static of large Pitot tube and wall cell; 43.3 inches of  $\frac{1}{2}$ -inch tubing; 93 ft./sec. Time breaks, 0.03 sec. apart. Wind tunnel motor, 695 revolutions per minute. Frequency of blade impulses, 46.3 per second

FIG. 19

yet been able to eliminate this oscillation, which entirely masks any pressure variation in the tunnel air stream.

This action is very pronounced even at low speeds when the damping is made small by using an impact opening. There seems to be a valvelike action of the gauge system, an impulse causing air to flow in; the impulse is transmitted to the gauge, reflected, and causes air to flow out. Owing to inertia there is an overshooting and the oscillation builds up and maintains itself.

A careful measurement of the wall cell record shows that there is an oscillation of small amplitude of a frequency of this order of magnitude, but we do not know its source.



## SUMMARY

Two methods of making studies of turbulence are described in this report, together with the results of their use in the 54-inch wind tunnel of the Bureau of Standards. The first method consists in measuring the drag of circular cylinders; the second, in measuring the static pressure at some fixed point. Both methods show that the flow is not entirely free from irregularities.

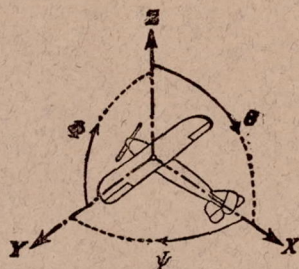
We have shown that the main fluctuations of static pressure in our 54-inch wind tunnel are associated with the unequal driving force over the tunnel mouth. There is a pattern of static pressure changes accompanying the propeller in its revolution. We have pointed out the difficulties encountered in attempting to make measurements by means of a Pitot tube connected to a sensitive gauge.

## BIBLIOGRAPHY AND REFERENCES

- Reference 1. *Ergeb. Aerodyn. Versuchsanstalt Gottingen I*, 1923, p. 24.
- Reference 2. *Scientific Paper 394*. By H. L. Dryden. Bureau of Standards, Sept., 1920.
- Reference 3. British Advisory Committee for Aeronautics, Reports and Memoranda No. 102—Discussion of the Results of Measurements of the Resistance of Wires, with Some Additional Tests on the Resistance of Wires of Small Diameter.
- Reference 4. *Physik. Zeitschrift*, Jan. 15, 1912. Karman.
- Reference 5. British Advisory Committee for Aeronautics, Reports and Memoranda No. 917—The Frequency of the Eddies Generated by the Motion of Circular Cylinders Through a Fluid. By E. F. Relf & L. F. G. Simmons. June, 1924.
- Reference 6. Rayleigh—Theory of Sound, chap. 16.
- Reference 7. On the Transmission of Air Waves Through Pipes. L. F. G. Simmons and F. C. Johansen. *Phil. Mag. S. 6*. Vol. 50. No. 297. Sept. 1925.
- Reference 8. Rayleigh—Theory of Sound, chap. 3—for mathematical theory.







Positive directions of axes and angles (forces and moments) are shown by arrows

Axis		Force (parallel to axis) symbol	Moment about axis			Angle		Velocities	
Designation	Sym- bol		Designa- tion	Sym- bol	Positive direction	Designa- tion	Sym- bol	Linear (compo- nent along axis)	Angular
Longitudinal----	X	X	rolling-----	L	Y → Z	roll-----	Φ	u	p
Lateral-----	Y	Y	pitching-----	M	Z → X	pitch-----	Θ	v	q
Normal-----	Z	Z	yawing-----	N	X → Y	yaw-----	Ψ	w	r

Absolute coefficients of moment

$$C_l = \frac{L}{q b S} \quad C_m = \frac{M}{q c S} \quad C_n = \frac{N}{q f S}$$

Angle of set of control surface (relative to neutral position),  $\delta$ . (Indicate surface by proper subscript.)

#### 4. PROPELLER SYMBOLS

Diameter,  $D$

Pitch (a) Aerodynamic pitch,  $p_a$

(b) Effective pitch,  $p_e$

(c) Mean geometric pitch,  $p_g$

(d) Virtual pitch,  $p_v$

(e) Standard pitch,  $p_s$

Pitch ratio,  $p/D$

Inflow velocity,  $V'$

Slipstream velocity,  $V_s$

Thrust,  $T$ .

Torque,  $Q$ .

Power,  $P$ .

(If "coefficients" are introduced all units used must be consistent.)

Efficiency  $\eta = T V/P$ .

Revolutions per sec.,  $n$ ; per min.,  $N$ .

Effective helix angle  $\Phi = \tan^{-1} \left( \frac{V}{2\pi r n} \right)$

#### 5. NUMERICAL RELATIONS

1 HP. = 76.04 kg/m/sec = 550 lb./ft./sec.

1 kg/m/sec = 0.01315 HP.

1 mi./hr. = 0.44704 m/sec

1 m/sec = 2.23693 mi./hr.

1 lb. = 0.4535924277 kg

1 kg = 2.2046224 lb.

1 mi. = 1609.35 m = 5280 ft.

1 m = 3.2808333 ft.